FORCE AND TRACTION CONTROLLED PROPULSION OF THE OMNIDIRECTIONAL WHEELED CLIMBING ROBOT CROMSCI

C. MARX, D. SCHMIDT*, C. HILLENBRAND and K. BERNS

Robotics Research Lab,
Department of Computer Science,
University of Kaiserslautern,
67653 Kaiserslautern, Germany
**E-mail: dschmidt@cs.uni-kl.de*
http://agrosy.cs.uni-kl.de/cromsci

Climbing on vertical concrete structures like bridge pylons or dams is still a great challenge for autonomous robots. This paper presents the force- and traction control system of the climbing robot CROMSCI which uses a negative pressure system for adhesion and driven wheels for propulsion. Especially in vertical environments the propulsion system must be able to produce enough force for carrying and accelerating the robot contrarily to gravity. Slippery of the wheels must be minimized due to abrasion and uncontrollable movements of the robotic system. This can be done by measuring upcoming forces and taking them into account for a traction control system (TCS). Another problem may occur because of slightly different wheel orientations which will result in increasing shear forces. We will show a control system to minimize these errors and experimental results which demonstrate its functionality.

Keywords: Climbing Robot, Wheeled Propulsion, Negative Pressure, Shear Force Control, Traction Control System, TCS.

1. Motivation and State of the Art

Service robots are used in many applications which might be dangerous or unreachable for humans. One of these is the inspection of concrete buildings which normally uses complex access devices like cranes or gondolas. Climbing robots can be used to fulfill this task (semi-)autonomously under survey of a technician and inspect a building area-wide and more safely.

There exist multiple kinds of propulsion and adhesion techniques of climbing robots in literature. The most common technology is to use passive suction cups [1]. Other methods use magnetic [2], van-der-Waals molecular

adhesion [3] or kind of claws [4]. These systems are not suitable to concrete walls because of the rough surface, missing ferromagnetic material or low payload. Beside electroadhesive methods [5] the negative pressure adhesion is the most confident technique for the proposed application, which is used by a couple of institutes around the world, e.g. [6] [7] [8]. Some of these systems only work on smooth surfaces or use legs or a sliding frame mechanism for locomotion which results in slow and rugged movement. An active vacuum system driven by omnidirectional wheels seems to be the best solution for climbing on concrete surfaces to achieve a fast and continuous motion and a more simple mechanical structure.

Nevertheless, wheeled system have the disadvantage of wearing due to wheelspin and lateral forces. This problem can be reduced by using a traction control system to minimize slippage and additionally improve odometry values. An overview concerning different traction control systems applied at automobiles can be found at [9].

2. Climbing Robot CROMSCI

The climbing robot Cromsci (see figure 1) combines a negative pressure system with active sealings and an omnidirectional drive for locomotion [10]. The round shape has a total height of $50cm$ and a diameter of $80cm$. On an outer ring a movable manipulator arm can be mounted which carries the sensors for inspection (e.g. cover meter or camera). The overall weight is at about $50kg$ including the manipulator arm with an additional payload of about $10kg$. The robot is connected via an umbilical cord to a ground station because of the high energy consumption and for communication purposes.

The negative pressure system consist of a large reservoir chamber evacuated by three suction engines and seven single vacuum chambers producing the adhesion force. Integrated sensors measure air pressures and allow a close-loop controlling via valves, which connect each working chamber to the reservoir. By these valves it is also possible to isolate single chambers with a high leakage area to avoid the propagation of normal pressure to the whole system. Additionally a thermodynamical model has been created to simulate the airflow and pressure propagation as well as to set up the close-loop controller. Beside the chambers a sealing system is needed which proofs the vacuum system to the environment to create enough negative pressure. For leak tightness Cromsci is equipped with an air filled tube in the shape of spokes which produces a constant force to the sliding area independent to the ground shape.

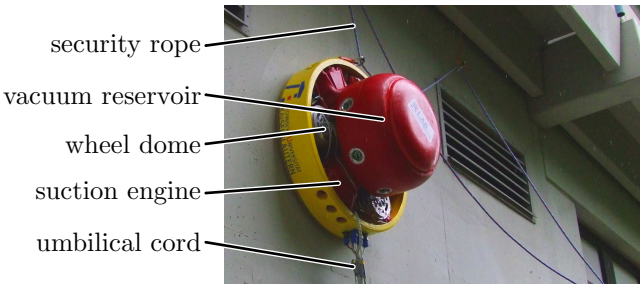

Fig. 1. Prototype CROMSCI (Climbing RObot with Multiple Sucking Chambers for Inspection tasks) driving at a concrete wall secured by a rope and supplied via umbilical cord (manipulator arm not mounted)

3. Propulsion System

For a high maneuverability CROMSCI uses three unsprung steerable and driven wheels (maximum speed of $9.63m/min$). The decision to build up an omnidirectional drive system results from special requirements like high maneuverability to reach all places on the building and high propulsion forces for movement. For driving curves but also driving sidewards and turning onto a point three degrees of freedom (DOF) are needed. The maneuverability δ_M can be described as the sum of mobility δ_m (DOF realized only by driving without changing the internal state) and steerability δ_s (additional DOF by steering the wheels). For CROMSCI these values result in $\delta_m = 1$ and $\delta_s = 2$.

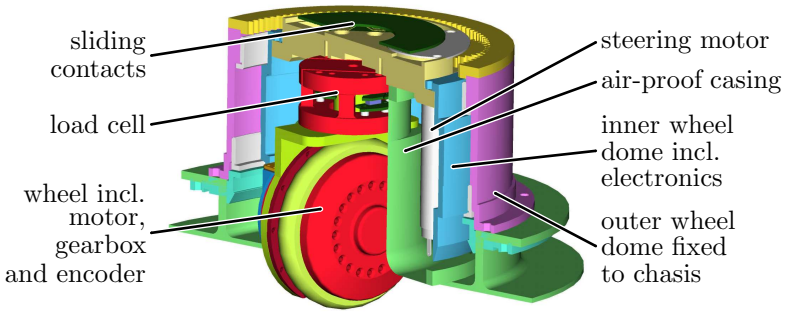

Fig. 2. The propulsion unit including wheel domes, load cell and inner wheel lying inside of an air-proof casing – the wheels are mounted inside of vacuum chambers

Each wheel (see figure 2) uses a combination of torque motor and Harmonic Drive and includes motor electronics, encoders and a load cell. An

additional DC motor is used for steering the wheel by turning the complete inner wheel dome. A load cell is integrated to measure one force and two torques at the contact point between wheel and wall. For the z-force up to 2000N and in the x/y-direction ± 400N can be detected.

3.1. *Traction Control System (TCS)*

In classic drive controllers as they are used in cars two ways exist to reduce the drive torque which is necessary for TCS. One can either influence the motor controller itself e.g. via throttle flap, ignition point or the amount of injected fuel or one can brake wheels selectively by using advanced hydraulics of an antilock brake system (ABS). But in contrast to a normal automobile the robot CROMSCI does not have any passive wheels which could be taken into account to measure a rotary velocity as reference. Therefore it is not possible to use a classic traction control based on slip values.

Instead of that CROMSCI uses a slip reduction technique based on measured forces of the load cells. These values lead via an estimated static friction value μ^{est} to a maximum amount $F_{i,x}^{max}$ of transferable force between each wheel i and wall in rolling direction. The wheel's propulsion is adjusted if the actual force in driving direction reaches a specific percentage of this maximum, which is calculated via actual downforce $F_{i,z}^{act}$ and affecting sideward force $F_{i,y}^{act}$ regarding equation 1. The Kammscher Circle in figure 3 shows the maximum transferable force.

$$F_{i,x}^{max} = \sqrt{\left(\mu^{est} \cdot F_{i,z}^{act}\right)^2 - \left(F_{i,y}^{act}\right)^2} \tag{1}$$

The traction control system of CROMSCI uses two steps for adjusting the wheel rotation. These steps result from the overall control structure based on a motor control system implemented on a digital signal processor. This close-loop controller using both proportional and integral proportion (PI) is able to adjust the motor velocity by changing the pulse-width modulation (PWM) value. The first step is now to trim the PWM maximum $I_{i,v}^{max}$ of wheel i by comparing actual $F_{i,x}^{act}$ and maximal force $F_{i,x}^{max}$ (eq. 2). The former PWM maximum $I_{i,v}^{max,old}$ is enhanced by update factors with $I^p << I^m$, which allow a quick limitation and a much slower regeneration. Afterwards $I_{i,v}^{max}$ is limited to the variable's boundaries.

$$I_{i,v}^{max} = \begin{cases} I_{i,v}^{max,old} - I^m \ , \text{ if } F_{i,x}^{act} > F_{i,x}^{max} \\ I_{i,v}^{max,old} + I^p \ , \text{ else} \end{cases} \tag{2}$$

This PWM maximum limits the motor velocity, but will lead to an increasing integral value of the motor controller. Therefore the integral proportion has to be adapted within the second step so that the absolute sum of proportional and integral value is not larger than the PWM maximum.

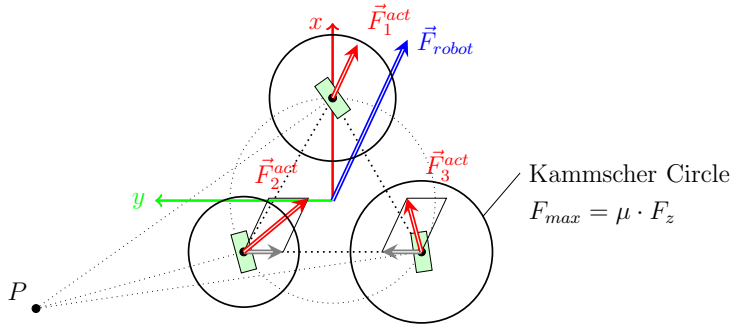

Fig. 3. Measured forces at different wheels and resulting total force. The circles show the maximum transferable force based on downforce F_z and friction μ. Both bottom wheels diverge and produce (horizontal) shear forces

3.2. *Shear Force Controlling (SFC)*

Beside the TCS an additional control of the wheel steering is needed to minimize contrarily orientations for reducing sideward forces which lower the transferable force $F_{i,x}^{max}$ as shown in eq. 1. These unmeant situations can occur because of steering transitions, incorrect initializing or runtime errors of the turning wheel domes. To reduce these shear forces the actual force values of each wheel $F_{i,x/y/z}^{act}$ and the current wheel orientation φ_i are used to calculate the desired forces for each wheel depending on the percentage of current downforce $F_{i,z}^{act}$ (with $i, j \in \{front, left, right\}$):

$$\begin{pmatrix} F_{i,x}^{des} \\ F_{i,y}^{des} \end{pmatrix} = \frac{F_{i,z}^{act}}{\sum_j F_{j,z}^{act}} \cdot R(-\varphi_i) \cdot \sum_j R(\varphi_j) \cdot \begin{pmatrix} F_{j,x}^{act} \\ F_{j,y}^{act} \end{pmatrix} \tag{3}$$

For adapting steering angles to reduce the forces in y-direction the new values are calculated regarding eq. 4 and 5 by using a PI-similar controller with amplification parameters $k_{P/I,\varphi}$ and an initial downforce F_z^{rob} which is one third of the robots weight. The forces in rolling direction can be reduced in the same way by calculating velocities v_i with parameters $k_{P/I,v}$ and by comparing forces in x- instead of y-direction.

$$\varphi_i = \varphi_i^{des} - k_{P,\varphi} \cdot \frac{F_z^{rob}}{F_{i,z}^{act}} \cdot \left(F_{i,y}^{des} - F_{i,y}^{act}\right) - k_{I,\varphi} \cdot \frac{F_z^{rob}}{F_{i,z}^{act}} \cdot I_{i,\varphi} \tag{4}$$

$$I_{i,\varphi} = I_{i,\varphi}^{old} + \left(F_{i,y}^{des} - F_{i,y}^{act}\right) \tag{5}$$

Figure 4 shows the setup of both controllers. The desired steering and driving commands are adapted by the SFC based on actual downforce values which are distributed as mentioned before. A motor controller generates PWM signals for the motors. Based on the estimated friction value and current forces the PWM of the motors for locomotion is limited by the TCS.

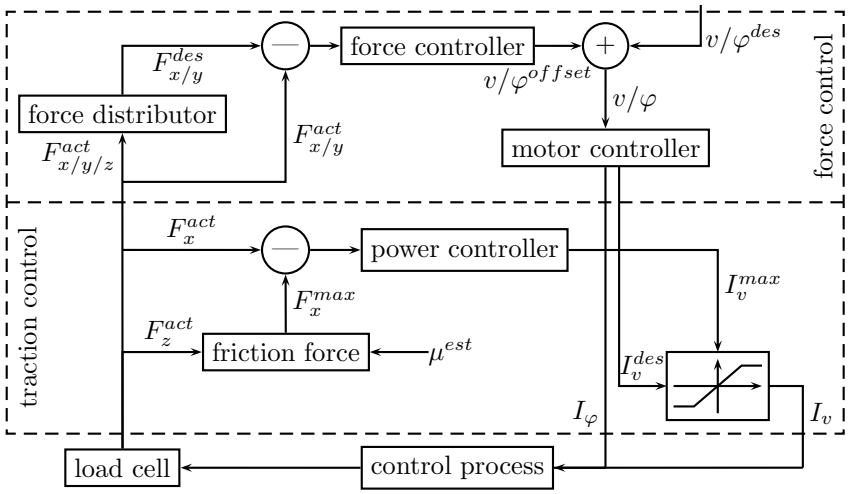

Fig. 4. Setup of combined shear force controller and traction control system (wheel indizes are left out for clearness)

4. Experimental Results

In contrast to vehicles moving horizontal wheeled climbing robots have to deal with high forces e.g. based on gravity and sealings friction. These forces have to be overcome by the locomotion system and results in high slippage values of up to 60-70%. Figure 5 shows the effect of immediate acceleration: If the traction control system is deactivated the wheelspin constrains the movement of the robot and it nearly stucks at the same position. In the other case the power of the wheel is adapted and the robot is able to move up to eight times farther. Nevertheless a general slippage as mentioned before can not be avoided via TCS while driving with a fixed velocity [11].

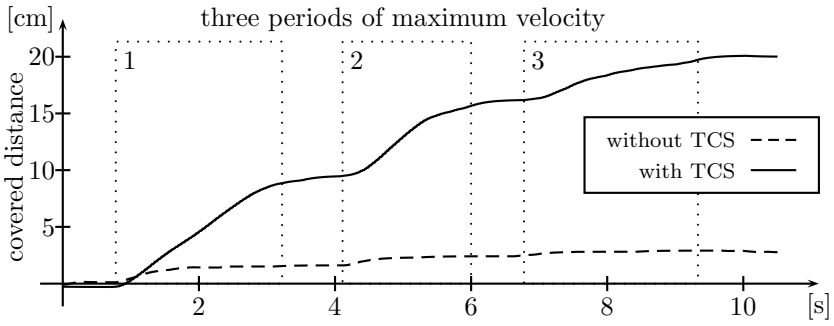

Fig. 5. The covered vertical distance with and without traction control system (TCS) performing stop-and-go at maximum velocity and acceleration three times

The results of the shear force controller are very promising. In figure 6 the lateral forces of the front wheel are shown with and without SFC while driving up a wall with changing velocities and directions heavily. It can be seen that the overall force is about 50% lower if the controller is activated but still reaches up to ±150N. The lateral force values of the lower wheels have not been enhanced that much as a result of a stronger dependency among themselves. In general the forces are distributed much more uniform.

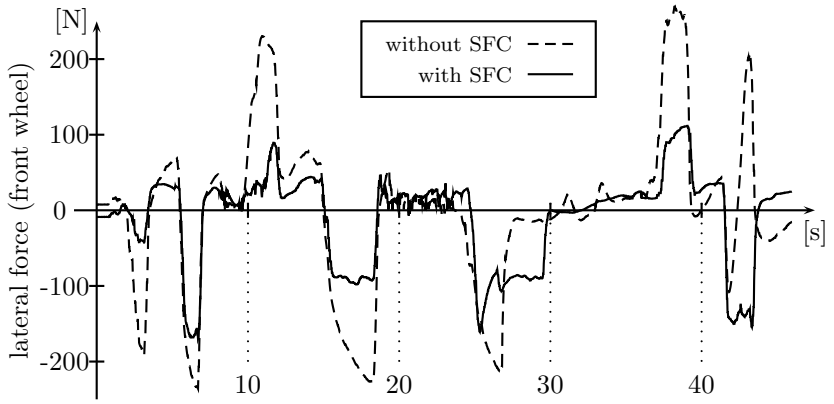

Fig. 6. The lateral forces of the front wheel while moving up a wall with permanently changing velocity and direction commands - with and without shear force control (SFC)

5. Conclusion

We presented a traction control system and a shear force controller of our climbing robot CROMSCI based on measured force values. The experimental results are very promising although a general slippage of up to 70% cannot be avoided to overcome gravity. This slippage can only be reduced by a more light-weighted robot, lower sealing and higher wheel friction by using other materials. The SFC works well but lacks of slow actuators for steering relative to the fast increasing shear forces. Future work lies in implementation of methods to get information about the robot's movement (e.g. INS, optical flow) and combine these with the introduced controllers.

References

1. N. Elkmann, M. Lucke and T. Krüger et al., Kinematics, sensors and control of the fully automated facade cleaning robot siriusc for the fraunhofer headquarters building munich, in *Climbing and Walking Robots*, July 2007.
2. W. Fischer, F. Tache and R. Siegwart, Magnetic wall climbing robot for thin surfaces with specific obstacles, in *6th International Conference on Field and Service Robotics (FSR)*, 2007.
3. S. Kim, M. Spenko and S. Trujillo et al., Whole body adhesion: hierarchical, directional and distributed control of adhesive forces for a climbing robot, in *IEEE International Conference on Robotics and Automation*, April 2007.
4. K. Autumn, M. Buehler and M. Cutkosky et al., Robotics in scansorial environments, in *SPIE - The International Society for Optical Engineering*, May 2005.
5. H. Prahlad, R. Pelrine and S. Stanford et al., Electroadhesive robots - wall climbing robots enabled by a novel, robust and electrically controllable adhesion technology, in *International Conference on Robotics and Automation (ICRA)*, May 19-23 2008.
6. H. Zhang, J. Zhang and G. Zong et al., Sky cleaner 3 - a real pneumatic climbing robot for glass-wall cleaning, in *IEEE Robotics And Automation Magazine*, March 2006.
7. D. Longo and G. Muscato, The alicia3 climbing robot, in *IEEE Robotics And Automation Magazine*, March 2006.
8. B. Luk, L. Liu and A. Collie, Climbing service robots for improving safety in building maintenance industry, in *Bioinspiration and Robotics: Walking and Climbing Robots*, September 2007 pp. 127–146.
9. M. Burckhardt, *Fahrwerktechnik: Radschlupf-Regelsysteme* (Vogel Buchverlag, 1993).
10. C. Hillenbrand, D. Schmidt and K. Berns, Cromsci - development of a climbing robot with negative pressure adhesion for inspections, in *Industrial Robot Volume 35 Issue 3*, (Emerald Group Publishing Ltd., May 13 2008).
11. C. Marx, Kraft- und traktionskontrollierte fortbewegung des omnidirektionalen kletterroboters cromsci, University of Kaiserslautern, (2009).